acta physica slovaca vol. 45 No. 6, 741 – 748 December 1995

FISSION COINCIDENT PRE-EQUILIBRIUM NEUTRON EMISSION FROM HEAVY-ION REACTIONS[1][2]

W. Scobel[3] and K. Knoche

I. Institut für Experimentalphysik, Universität Hamburg, D-22761 Hamburg, Germany

Received 23 October 1995, accepted 27 October 1995

Binary fragmentations from the reactions $^{19}F + ^{209}Bi$ (E_p = 491 MeV) and $^{64}Ni + ^{165}Ho$ (E_p = 778 MeV) leading to highly excited composite nuclei with similar masses were investigated by measurement of the fission coincident neutrons. The pre-equilibrium (PE) component was separated with a moving source analysis from pre– and postscission contributions and studied as a function of the linear momentum transferred. PE neutrons from the reaction $^{19}F + ^{209}Bi$ exhibit a significant out–of–plane anisotropy whose neglection would result in an overestimation of the PE neutron multiplicity by more than 30%. The PE multiplicities and temperature parameters for the more symmetric entrance channel $^{64}Ni + ^{165}Ho$ indicate a delay in fusion, which is typical for fast fission and in agreement with the observed asymmetric mass splits.

1. Introduction

The dissipation of energy, mass, and angular momentum in heavy ion induced reactions can be studied with fission coincident light particle emission. For projectile energies below 10 MeV/u a low mass asymmetry in the entrance channel leads to fusion times in the order of evaporation time scales and observable implications.For higher projectile energies fusion and equilibration times can become comparable. The influence of dynamical delays in fusion of mass symmetric entrance configurations may then be studied with reference either to model calculations neglecting such effects, or to much more mass asymmetric systems. The latter way is particularly useful, because absolute values of time scales obtained e.g. from moving source analyses are not free from systematic errors [1, 2].

In the present work we study fission coincident prequilibrium (PE) neutron emission following central collisions in the two entrance channels $^{19}F + ^{209}Bi$ and $^{64}Ni + ^{165}Ho$ of

[1] Dedicated to M. Blann on the occasion of his 60th birthday

[2] Presented at the International Symposium on Pre-Equilibrium Reactions, Smolenice Castle, 23 – 27 October, 1995

[3] E-mail address: SCOBEL@KAA.DESY.DE

highly different mass asymmetry, angular momentum population and linear momentum transfer, but similar composite mass A ≈ 228 and excitation energy E* ≈ 390 MeV. The observed entrance channel effects are qualitatively discussed in the framework of the Boltzmann master equation (BME) model.

2. Experimental setup and procedure

The experiment was performed with ^{64}Ni and ^{19}F projectiles of energies 778 MeV (i. e. 12.2 MeV/u) and 491 MeV (26.1 MeV/u),respectively, from the VICKSI facility at the Hahn–Meitner Institut,Berlin, that operated with burst widths $\Delta t = 0.9$–1.2 ns. The detector setup for the ^{19}F + ^{209}Bi experiment is shown in Fig. 1. Fission fragment (FF) like reaction products were registered with low–pressure multiwire chambers (MWC) and surface barrier detectors (SB). The MWC's were centered around the angles $\Theta_{MWC} = \pm 68°$ (for ^{64}Ni+ ^{165}Ho : 42°), which correspond to the most probable linear momentum transfer (LMT) of 78% (95%) for symmetric fragmentation [3]. Their detection efficiencies extended to 20% and beyond 100% LMT, respectively, the out–of–plane acceptance $\Delta\Psi$ to $\pm$ 13°.

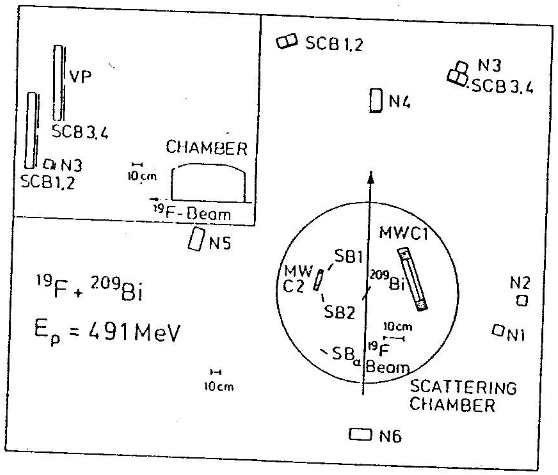

Fig. 1. Experimental setup consisting of position sensitive multiwire chambers (MWC$_i$) and solid state detectors (SB$_i$)inside the scattering chamber, liquid scintillators N$_i$ (some with veto paddles VP) and position sensitive scintillator bars (SCB$_i$) for neutron detection. The inset gives a side view.

For neutron time–of–flight (TOF) spectroscopy we used up to 10 cylindrical cells filled with liquid scintillator materials NE213 or BI501. The γ–background was reduced with sheets of lead in front of the cells, and with pulse–shape techniques; charged particles were identified with thin scintillator veto paddles (VP) in front. The cells were positioned at reaction angles Θ_{lab} ranging from 0° to 163° within as well as outside the reaction plane. In the ^{19}F + ^{209}Bi experiment, this setup was supplemented [4] by four plastic scintillator bars (SCB) of size $10 \times 10 \times 100$ cm^3 made from BC408. They were installed perpendicular to the reaction plane (see Fig.1) and covered out–of–plane angles Ψ up to 45° for a consistent measurement of relative neutron angular distributions in this direction. The bars were read out on both sides to deduce the position of neutron incidence with the time difference technique. The position resolution was $\Delta x \leq 5$ cm (FWHM). For experimental reasons [4], the analyzed detector volume was restricted to 5 cm $\leq x \leq$ 95 cm and treated as nine bins of 10 cm length.

Special efforts were made to obtain consistent values for the neutron detection efficiency ϵ_n of both, scintillator cells and bars. For the cells, ϵ_n was calculated with the code of Cecil *et al.* [5]. The efficiency of the bars was determined experimentally with reference to the cell N3 of size 10.4 cm diameter and 10.4 cm thickness that was placed in a position homologous to a section of SCB2, see Fig. 1. The experimental efficiencies turned out to be higher than those calculated with [5] for a cubic scintillator bar segment, but were in agreement with efficiencies obtained with neutrons from spontaneously fissioning ^{252}Cf [4]. Therefore the calculated efficiency normalized with a factor 1.12 to the experimental result (cf. Fig. 2) was applied to the scintillator bars. Further experimental details are given in [6].

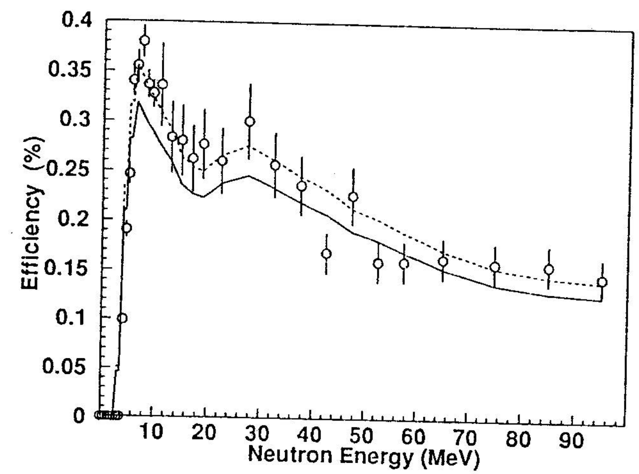

Fig. 2. Neutron detection efficiency from comparison of scintillator bar segment with liquid scintillator cell (o), from Monte Carlo simulation [5] (solid line), and after normalization (dashed).

3. Data analysis

The analysis of the fragment observables assumes a binary fragmentation following a massive transfer of a fraction of the projectile mass; the remainder proceeds as spectator with projectile velocity. The LMT to the recoiling composite system is then

$$LMT = \frac{v_{\|}}{v_0} \frac{1}{1 + \frac{m_p}{m_T}(1 - \frac{v_{\|}}{v_0})} \quad (1)$$

where $v_{\|}$ denotes the recoil velocity in beam direction, v_0 its maximum value occurring for complete fusion, m_p and m_T projectile and target mass, respectively. The recoil velocity $v_{\|}$ is calculated from the observed fragment velocities v_1, v_2, their angles Φ_1, Φ_2 with respect to the projectile direction (i.e. $\cos\Phi = \cos\Theta \cos\Psi$), and the folding angle Φ_{12} between $\vec{v_1}$ and $\vec{v_2}$.

The fragment masses m_i/m_{CN}, i=1,2 in units of mass $m_{CN} = m_T + LMT \times m_p - m_{evap}$ remaining after particle evaporation will be furtheron referred to as *normalized* mass M_N. The mass correction m_{evap} was calculated with a statistical model starting at the excitation energy E^*_{CN}(LMT) $\propto$ LMT remaining after equilibration [7]. In the analysis the events were subdivided into symmetric ($0.4 \leq M_N \leq 0.6$) and asymmetric fragmentations and into the intervals ΔLMT as indicated in Fig. 3. The contour diagrams in the LMT vs. M_N plane show characteristic differences:

The ^{64}Ni induced process favours central collisions (cc) with an almost complete LMT; in rare cases, peripheral collisions with $\approx$ 30% LMT occur. The most probable LMT of 98% agrees well with existing systematics [3]. Despite the high excitation energies $E^* > 300$MeV, however, the asymmetric fragmentations prevail. The total kinetic energies (TKE) carried away by these fragments exceed those expected for full dissipation of the projectile energy into dissipation, cf. Fig. 3. The yield under the cc peak, corrected for the detector efficiency, can be converted into a total cross section σ_{cc} and an associated sharp cut off angular momentum l_{cc} , that turned out to be 134$\hbar$. This is not far above the critical value $l_{crit} = 120\hbar$ for a vanishing potential pocket in fusion [8]. The depletion of the difference Δl is essentially accounted for by PE emission that is also responsible for the fraction of linear momentum *not* transferred. According to the rotating liquid drop model (RLDM), the fission barrier vanishes already for $l_0 = 67\hbar$. Therefore central collisions proceed primarily through exit channels with *no* fission barrier and this is what we observe in Fig. 3.

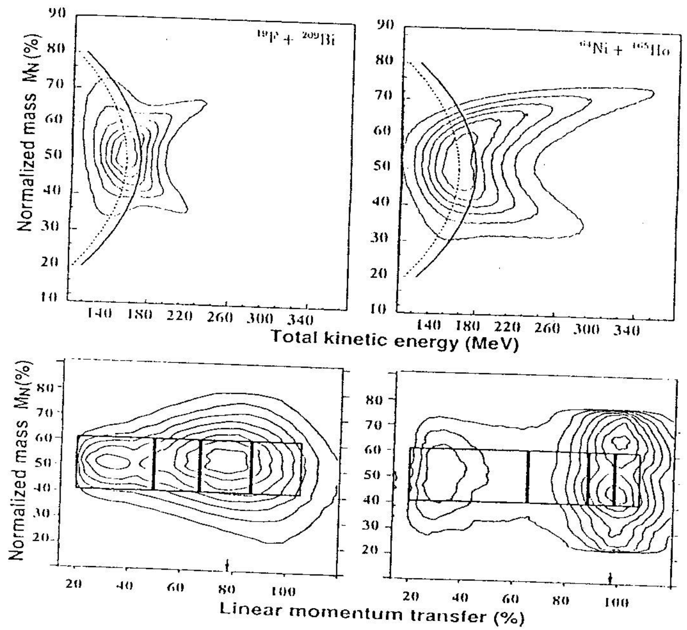

Fig. 3. *Top:* Contour diagram of total kinetic energies TKE vs. normalized mass M_N; increase of yield is 14% between adjacent lines. Also shown the TKE's calculated after [3] for all mass splits, both without (solid line) and with (dotted) particle emission preceding scission. *Bottom:* Contour plot of LMT vs. M_N corrected for detection efficiency; increase of yield is 11% from line to line. The boxes indicate the different fragmentation classes of the analysis.

The ^{19}F induced process shows a pattern known from several fusion–fission reactions with projectiles in this mass and energy/nucleon range. The most probable LMT is 78% and the preferred fission mode is the symmetric one. The observed TKE values in the upper part of Fig.3 support the interpretation of an equilibrated system. Integration of the cc peak yields a cross section σ_{cc} that converts into $l_{cc} = 123\hbar$. This is substantially higher than the value $l_{crit} = 82\hbar$ for fusion or even $l_0 = 74\hbar$ where the RLDM fission barrier vanishes. In the ^{19}F induced reaction therefore most of the central collisions lead to a fusion–fission sequence of these highly fissile ($x \approx 0.8$) composite systems. The 22% of linear momentum not transferred convert [9] into a depletion $\Delta l = 40\hbar$ of angular momentum in PE emission, in perfect agreement with the difference $l_{cc} - l_{crit} = 41\hbar$.

From these considerations we expect the ^{64}Ni induced reaction to show little PE neutron emission in fission coincidences, whereas it should be substantially higher for ^{19}F + ^{209}Bi. Direct evidence must be extracted from the neutron spectroscopy itself. The double differential multiplicities $M_n(E_n, \Theta_{lab})$ of fission-coincident neutrons were analyzed separately for each of the different LMT and M_N classes with a moving source fit. The decomposition considered contributions from a pre-equilibrium (PE) and a compound nucleus (CN) source, and two sources of fully accelerated fragments (F1, F2). Each one was supposed to emit isotropically in its own rest frame. The resulting total double–differential neutron multiplicity in the laboratory frame is thus given by

$$\left(\frac{d^2M_{tot}}{dE_n d\Omega}\right)_{lab} = \sum_{i=1}^{4} \frac{M_{n,i}}{2(\pi T_{n,i})^{\frac{3}{2}}} \sqrt{E_n} \times \exp\left[-\frac{E_n + \epsilon_i - 2\sqrt{E_n \epsilon_i} cos\Theta_i}{T_{n,i}}\right] \quad (2)$$

Here, $M_{n,i}$ denotes the neutron multiplicity and ϵ_i the kinetic energy per nucleon of the ith source. The temperature parameters T_i are averaged over the whole emission cascade of the respective source. The emission angle Θ_i refers to the velocity direction of each source. Free fit parameters were the multiplicities $M_{n,i}$ and temperatures T_i for all four sources, and the kinetic energy ϵ_{PE} of the PE source. The velocities of the CN and the fragment sources were deduced from the data.

Representative sets of decompositions for the most probable LMT bin and symmetric fragmentations are shown in [6]. The best fit values for the PE neutron multiplicity $M_{n,PE}$ are 1.1 ± 0.9 neutrons per fission for ^{64}Ni+^{165}Ho and 3.0 ± 0.5 for ^{19}F + ^{209}Bi. The latter result does not only confirm the anticipated higher PE neutron multiplicity; it is also more pronounced due to the harder spectral shape (see Table 1) and therefore much better separable from the three equilibrium sources (which are discussed in detail in [6]). This is why the out–of–plane study was restricted to the system ^{19}F + ^{209}Bi.

Reaction	E_{proj}	$\frac{E_{cm}-V_C}{A_p}$	$n_0^\dagger$	$n_0^\ddagger$	n_0	$M_{n,PE}$	$LMT(\%)$	$E_{kin,n}$
^{19}F + ^{209}Bi	491	19.3	23	25	19(24)	3.0(2.2)	81(88)	15(12.5)
					exp :	3.0 ± 0.5	78	12.2 ± 2
^{32}S + ^{197}Au	838	18.3	37	41	32(41)	4.6(3.1)	79(87)	14.3(11.7)
					exp :	4.1 ± 0.3	74	12.0 ± 0.8
^{64}Ni + ^{165}Ho	778	5.8	38	52	64(52)	1.4(2.7)	96(93)	6.5(7.5)
					exp :	1.1 ± 0.9	98	7.8 ± 2

Table I. Values n_0 from [10]†, [11]‡, and comparison of experimental data $M_{n,PE}$, most probable LMT, and $E_{kin,n}$ with BME calculations for two sets of n_0. Energies in MeV.

4. PE neutron distributions

Our discussion will be restricted furtheron to the central collisions which are associated to the most probable LMT with symmetric fragmentations. The fit results, including those for ^{32}S + ^{197}Au from [7], are listed in Table 1. The temperature parameters are converted into average kinetic energies $E_{kin,n} = \frac{3}{2}T_{n,PE}$.

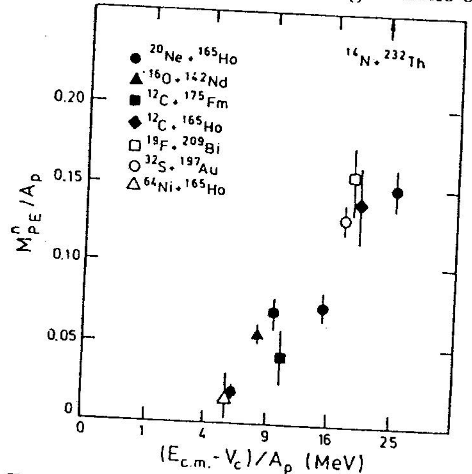

Fig. 4. Compilation [12] of PE neutron multiplicities together with data of this work (open symbols).

Fig. 4 shows that our results for $M_{n,PE}$ per fission agree well with recent systematics [12] and confirm their almost linear increase with the relative velocity v_r at the contact configuration (where the Coulomb barrier is of height V_C). It has been shown [3], that the LMT is a function of v_r, too, and independent from the projectile–target combination. Therefore v_r seems to control the extent PE emission decrements linear momentum and angular momentum.

The reaction plane defined by the emitted fission fragments is perpendicular to the spin of the CN. In this plane, all PE angular distributions are well described with eq.2; the velocity $v_{PE} = \sqrt{2\epsilon_{PE}/m_{nuc}}$, was in all cases about 50% of the projectile velocity [6, 13]. It is, however, not possible to describe the out-of-plane results, where the PE multiplicities decrease more rapidly for increasing angle (with respect to the beam direction) than observed *in* the reaction plane. Fig. 5 shows that, for large out-of-plane angles Ψ, this effect is drastic. For the description of this PE-anisotropy we have adopted [13] a factorized ansatz with an additional fit parameter a_n, viz.

$$M_{PE}(\Theta, \Delta) = M_{PE}(\Theta)\exp(-a_n cos^2\Delta) \qquad (3)$$

that replaces the PE term in Eq. (2) and reduces to it for $a_n = 0$. The best fitting values a_n vary with LMT class between 1.1 and 1.4. Already $a_n = 1.1$ would lead a measurement restricted to the reaction plane to an overestimation of the PE multiplicity of 37%! Even higher anisotropies were observed in ^{12}C induced reactions [13] though on a much lower absolute level. It is obvious that a neglect of this effect adversely influences the determination of time scales from neutron multiplicities. This anisotropic PE emission is intimately connected to the angular momentum depletion by $\Delta l \approx 40\hbar$ necessary to reach the limit $l_{crit} = 82\hbar$ for fusion: The composite nucleus must reduce its angular momentum during the early stages of its evolution towards this relative stability limit, and PE emission in directions perpendicular to the spin of the subsequently fissioning system is most effective in this respect.

The equilibration in central collisions by PE nucleon emission has been described [9] with the BME model. An important parameter therein is the initial number of degrees of freedom, n_0. As a first guess, n_0 may be identified with the number A_p of projectile nucleons. Empirical values have been derived from a fit of inclusive proton energy spectra for a range of projectiles and targets to BME calculations [11]. The trend of the resulting values for n_0 has been reproduced in microscopic calculations analyzing the geometric overlap of the colliding heavy ions [10]. These two methods yield values n_0 for our reactions that differ from A_p, see Table 1. We have performed BME calculations with them as well as with $n_0 = A_p$.

The choice of A_p leads to fair agreement for $M_{n,PE}$ and LMT, but not for $E_{kin,n}$. A better reproduction of the average kinetic energy is of course obtained with the values n_0 from the empirical systematics, because it was made to fit spectral shapes, i.e. distributions of $E_{kin,n}$. The agreement, however, goes together with an increasing discrepancy in $M_{n,PE}$ and LMT, that is of opposite sign for the more mass asymmetric entrance channels on one hand and ^{64}Ni + ^{165}Ho on the other, the latter being more pronounced. It indicates that for ^{64}Ni the BME model may be stretched beyond its limit of applicability.

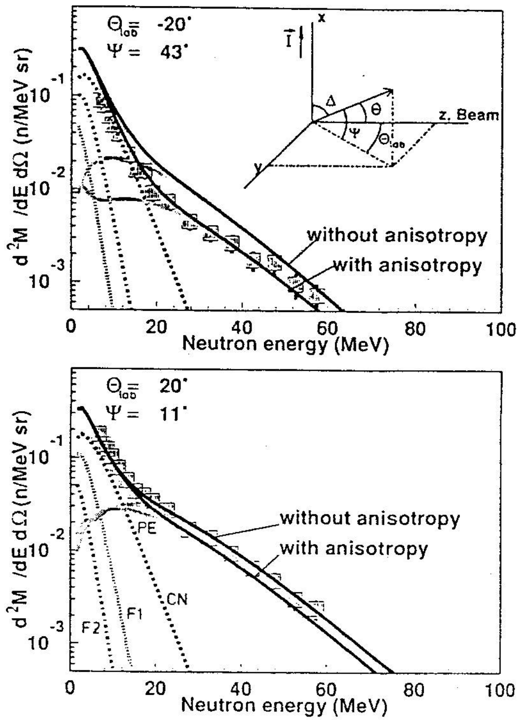

Fig. 5. Double differential neutron multiplicities for ^{19}F + ^{209}Bi (most probable LMT, symmetric fragmentation). Top (Bottom): Maximum (Minimum) out-of-plane position covered with the position sensitive SCB's. Fits are without and with anisotropy (eq.3). The solid line denotes the sum of the four sources CN, F1, F2, PE.

One reason is that heavy projectiles require long fusion times τ_{fus}; for ^{64}Ni, τ_{fus} amounts to 50% of the equilibration time τ_{eq}, whereas it is only 20% for the reference projectile, ^{19}F. Any additional delay during fusion slows the *increase* $dM_{n,PE}/dt$ and the *decrease* $dE_{kin,n}/dt$ down and causes for the ^{64}Ni reaction accordingly a lower $M_{n,PE}$ and a higher $E_{kin,n}$ and thus a better agreement of the BME calculation with the experiment.

The additional delay is supposed to be of dynamic origin. A delay of full equilibration in the even more mass symmetric entrance channel ^{64}Ni + ^{100}Mo has been reported [14], that, due to the lower projectile energy of 3.6 MeV/u, led to fusion times comparable to those for neutron evaporation and thus took influence on the evaporation process. In our case the fusion time scale merges with that for PE emission, because the kinetic energy in the entrance channel ^{64}Ni + ^{165}Ho is dissipated, before a spherical CN configuration is reached. The system therefore enters the exit channel, before mass equilibration is completed. Beyond the effect on the PE emission, the reaction ^{64}Ni + ^{165}Ho also favors a fast fission process with asymmetric fragmentation (cf. Fig. 3) and comparatively small pre- and large postfission neutron multiplicities as contrasted against the reference system ^{19}F + ^{209}Bi, [7].

5. Summary

Neutron spectroscopy has been performed in coincidence with binary fragmentations for composite systems of similar masses and energies, but different mass asymmetries and angular momenta in the entrance channel. For ^{19}F+^{209}Bi central collisions with symmetric fragmentations prevail. The angular momentum population exceeds the fusion stability limit considerably. It is depleted by PE emission that is therefore concentrated in a plane perpendicular to the total angular momentum, i. e. in plane with the fission fragments. The out-of-plane asymmetry is described with the parameter a_n ranging from 1.1 to 1.4.

Central collisions of ^{64}Ni + ^{165}Ho yield mass splits that are more asymmetric than the reference reaction. The discrepancy of the PE parameter set n_0, $M_{n,pre}$, $E_{n,kin}$ to calculations involving the BME model qualitatively indicates a delayed fusion. For more quantitative explanations, calculations are needed that combine the dynamics of nucleus-nucleus collisions with time-dependent statistical cascade calculations [2, 15].

Acknowledgements This work has been supported in part by the Bundesministerium für Bildung und Wissenschaft under contract 06HH561,Tp2.

References

[1] M. Blann *et al.*: *Phys. Rev. C* **37** (1988) 2231
[2] K. Siwek-Wilczynska *et al.*: *Phys. Rev. C* **51** (1995) 2054
[3] V. Viola: *Nucl. Phys. A* **502** (1989) 531
[4] L. Lüdemann *et al.*: *Nucl. Instrum. Methods Phys. Res. Sect. A* **334** (1993) 495
[5] R. A. Cecil *et al.*: *Nucl. Instr. Meth.* **171** (1979) 439
[6] K. Knoche *et al.*: *Phys. Rev. C* **23** (1995) 2711908
[7] E. Mordhorst *et al.*: *Phys. Rev. C* **43** (1991) 1908
[8] R. Bass: *Nucl. Phys. A* **213** (1974) 45
[9] M. Blann: *Phys. Rev. C* **31** (1985) 1245
[10] N. Cindro *et al.*: *Phys. Rev. Lett.* **66** (1991) 868
[11] M. Korolija *et al.*: *Phys. Rev. Lett.* **60** (1988) 193
[12] H.K.W. Leegte *et al.*: *Phys. Rev. C* **46** (1992) 991
[13] W.P. Zank *et al.*: *Phys. Rev. C* **33** (1986) 519
[14] M. Thoennessen *et al.*: *Phys. Rev. Lett.* **70** (1993) 4055
[15] E. Strumberger *et al.*: *Nucl. Phys. A* **529** (1991) 522